Mon. Not. R. Astron. Soc. **384,** 1649–1656 (2008) doi:10.1111/j.1365-2966.2007.12815.x

The periodicity of the η Carinae events⋆†‡§¶

A. Damineli,[1]‖ D. J. Hillier,[2] M. F. Corcoran,[3,4] O. Stahl,[5] R. S. Levenhagen,[1] N. V. Leister,[1] J. H. Groh,[1] M. Teodoro,[1] J. F. Albacete Colombo,[6] F. Gonzalez,[7] J. Arias,[8] H. Levato,[7] M. Grosso,[7] N. Morrell,[9] R. Gamen,[7] G. Wallerstein[10] and V. Niemela⋆⋆

[1]*Instituto de Astronomia, Geofísica e Ciências Atmosféricas, Universidade de São Paulo, Rua do Matão 1226, Cidade Universitária, São Paulo 05508-900, Brazil*
[2]*Department of Physics and Astronomy, University of Pittsburgh, 3941 O'Hara Street, Pittsburgh, PA 15260, USA*
[3]*CRESST and X-ray Astrophysics Laboratory, NASA/GSFC, Greenbelt, MD 20771, USA*
[4]*Universities Space Research Association, 10211 Wincopin Circle, Suite 500 Columbia, MD 21044, USA*
[5]*ZAH, Landessternwarte, Königstuhl 12, D-69117 Heidelberg, Germany*
[6]*UNLP – Facultad de Ciencias Astronomicas y Geofisicas de La Plata (FCAGLP), Buenos Aires, Argentina*
[7]*Complejo Astronomico El Leoncito, Casilla de Correo 467, San Juan, Argentina*
[8]*Departamento de Física, Universidad de La Serena, Chile*
[9]*Las Campanas Observatory, Carnegie Observatories, Casilla 601, La Serena, Chile*
[10]*Department of Astronomy, University of Washington, Seattle, WA 98195, USA*

Accepted 2007 December 5. Received 2007 November 1; in original form 2007 August 7

ABSTRACT

Extensive spectral observations of η Carinae over the last cycle, and particularly around the 2003.5 low-excitation event, have been obtained. The variability of both narrow and broad lines, when combined with data taken from two earlier cycles, reveal a common and well-defined period. We have combined the cycle lengths derived from the many lines in the optical spectrum with those from broad-band X-rays, optical and near-infrared observations, and obtained a period length of $P_{\rm pres} = 2022.7 \pm 1.3$ d.

Spectroscopic data collected during the last 60 yr yield an average period of $P_{\rm avg} = 2020 \pm 4$ d, consistent with the present-day period. The period cannot have changed by more than $\Delta P/P = 0.0007$ since 1948. This confirms the previous claims of a true, stable periodicity, and gives strong support to the binary scenario. We have used the disappearance of the narrow component of He I 6678 to define the epoch of the Cycle 11 minimum, $T_0 =$ JD 245 2819.8. The next event is predicted to occur on 2009 January 11 ($\pm$2 d). The dates for the start of the minimum in other spectral features and broad-bands are very close to this date, and have well-determined time-delays from the He I epoch.

Key words: stars: general – stars: individual: eta Carinae – stars: binary.

1 INTRODUCTION

η Carinae is one of the most-luminous stars in the Milky Way and contains many mysteries. It has been attracting attention since the 1820s, when it suffered large brightness fluctuations, culminating with the giant eruption that ejected the Homunculus in 1843. The star faded to naked eye invisibility, and after the discovery of the supernovae in the XIXth century it was classified as a slow supernova. However, around 1940, it started to brighten again, indicating that the star was only hidden by dust, not destroyed.

The spectrum is rich in emission lines of low-excitation species: H I, Fe II, [Fe II], [Ni II], Ti II, etc. (Thackeray 1953); after 1944 (Gaviola 1953) high-excitation forbidden lines of [Ne III], [Ar III], [S III] and [Fe III] can also be readily identified (see also Damineli et al. 1998, and references therein). Today, we know that the narrow lines (forbidden and permitted) are emitted in the Weigelt blobs (Weigelt & Ebersberger 1986), at ∼0.3 arcsec from the central star (Davidson et al. 1995) and the broad emission lines are formed in the wind of the central object (Hillier & Allen 1992; Davidson et al.

⋆Based partially on data collected at the OPD-LNA/MCT.
†Based partially on data collected at ESO telescopes.
‡Based partially on data collected at the Casleo Observatory.
§Based partially on data collected at Magellan Telescopes.
¶Based partially on data collected at CTIO.
‖E-mail: damineli@astro.iag.usp.br
⋆⋆Deceased

1995). The combination of high- and low-excitation lines in the same object, however, was paradoxical.

A key to understanding this interesting object was found recently through the study of the variability of the high-excitation lines. The high-excitation forbidden lines disappeared temporarily in 1948, and again in 1965, 1981, 1987 and 1992. These 'spectroscopic events' (Gaviola 1953; Rodgers & Searle 1967; Thackeray 1967; Zanella, Wolf & Stahl 1984) or 'low-excitation events' (Damineli et al. 1998) were believed to be part of S Doradus cycles, commonly seen in other Luminous Blue Variable stars similar to η Carinae. This interpretation seemed to be supported by the He I λ10830 line which went to minimum (Damineli 1996) when the near-infrared light curve went to maximum (Whitelock et al. 1994). The maxima in the near-infrared light curves were not truly periodic and the length of the quasi-period was different for different pass-bands. However, the spectroscopic events were demonstrated to be periodic (Damineli et al. 2000), in contrast to the incoherent character of the S Doradus oscillations. Damineli, Conti & Lopes (1997) and others proposed a binary model with a highly eccentric orbit, a hotter secondary component and a strong wind–wind collision (WWC). Binarity is interesting as it potentially allows the direct measurement of the mass of the stars, their most fundamental parameter. The binary scenario has provided a framework for understanding the star and provided guidelines for fruitful observations, although some prefer a model in which there are periodic shell ejections (Martin et al. 2006). In Fig. 1, we present examples of high- and low-excitation-state spectra of η Carinae.

The observation of an event in 1997.95, as was predicted, brought more confidence to the true periodic nature of the variation (Damineli et al. 2000). Feast, Whitelock & Marang (2001) used archival spectra to identify three previously unreported events, in 1953, 1959 and 1970, which also fit the 5.5-yr period. Moreover, those authors discovered that the dips on top of the broad quasi-periodic near-infrared maxima were truly periodic and correlated with the behaviour of the high-excitation lines. An extensive X-ray-monitoring campaign was started in 1996 with the *RXTE* satellite and revealed deep minima in 1997.95 and 2003.49 which coincided with the minima seen at other wavelengths (Corcoran 2005). X-ray observations inside and outside the minimum performed with *Chandra* and *XMM* furnished details on the column density ($N_{\rm H}$), temperature and chemical composition of the colliding wind shock (Hamaguchi et al. 2007). van Genderen et al. (2006) showed that the optical light curve displays periodic dips like those in the near-infrared and Lajús et al. (2003) reported a very detailed light curve in the B, V, R and I bands for the 2003.49 event. The events were recorded also at radio-cm (Duncan & White 2003) and radio-mm (Abraham et al. 2005), but no specific value to the period length was reported for those wavelengths.

Many other features vary periodically in intensity and radial velocity, like the broad emission and P Cygni absorption components, and can also be used to derive the period length. One of them is He II λ4686 discovered by Steiner & Damineli (2004), which raises and drops just before minimum faster than any other feature over the entire spectrum. Although faint [equivalent width (EW) < 2 Å] it was frequently monitored with high signal-to-noise ratio (S/N) along the last event. Unfortunately, it was observed only occasionally in the previous events, precluding its use to measure the period. This spectral line deserves better monitoring in future events, not only to improve the accuracy of the derived period, but also because it is the highest-excitation feature observed at optical wavelengths, and its origin remains a mystery.

To facilitate discussion, we label the events by numbers as described by Groh & Damineli (2004): number one (#1) is assigned to the event observed in 1948 by Gaviola, so that the event of 2003.49 is #11. We define *cycle* as the time-interval between the starting of two consecutive minima, so that cycle #9 started at the 1992.42 minimum and finished when cycle #10 was starting in 1997.95. Because of observational reasons, that will become clear later in this paper, the starting point of a cycle is defined by the disappearance of the He I λ6678 narrow-line component. With this definition, phases along the cycle are defined in a unique way for all measured quantities.

This paper is organized as follows. We present in Section 2 the observations, in Section 3 the definition of phase 0 of the minimum, in Section 4 the determination of the period length, in Section 5 the stability of the period, in Section 6 the relation between the sharp peaks during the giant eruption and periastron passages, and in Section 7 the discussion and conclusions.

2 OBSERVATIONS AND MEASUREMENTS

The majority of the ground-based observations presented in this paper came from a monitoring campaign started in 1989 at the Coudé focus of the 1.6-m telescope of the Pico dos Dias Observatory (OPD-LNA/Brazil). The observational set-up at OPD was kept

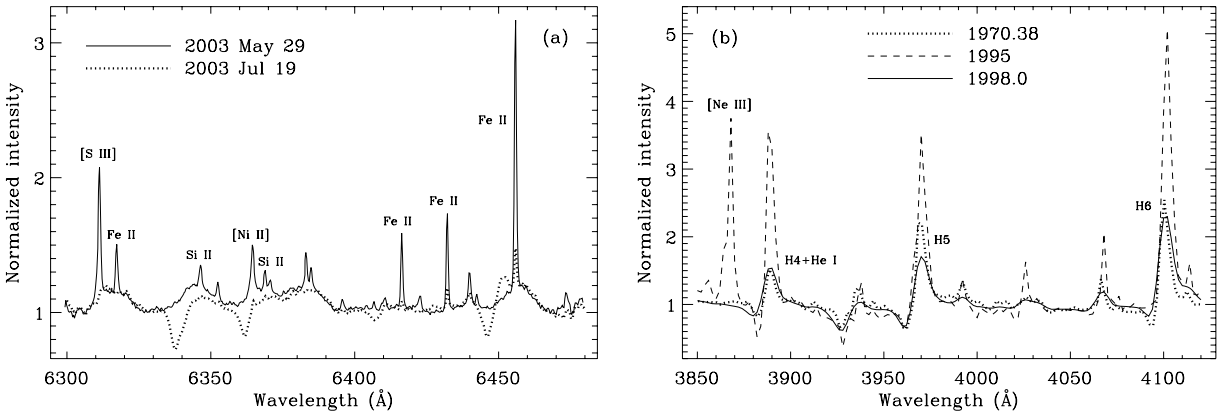

Figure 1. Sample of the η Carinae spectra at high- and low-excitation states. (a) High-resolution red spectrum showing the disappearance of narrow emission lines and strengthening of P Cygni absorption components during the minimum. (b) Low-resolution blue spectra showing the high state in 1995 and two spectra during the minimum taken on 1997 December 31 and 1970 May 17.

essentially unchanged through the campaign: a dispersion grating with 600 l mm^{-1}, entrance slit-width ∼1.3 arcsec, and exposure time ∼5 s in Hα increasing to ∼15 min at 3500 and 10 800 Å. Spectra were extracted along ∼2 arcsec in the spatial direction and no measurable differences in line intensities were seen when changing the extraction size by a factor of 2. Three different CCDs have been used, with resolving powers $R = 25$ km s^{-1} (0.25 Å pixel^{-1}) at Hα in 2003 and $R = 50$ km s^{-1} (0.39 Å pixel^{-1}) in the preceding years. On some occasions, a 1024 × 1024 Hawaii detector was used to observe the He I λ10830 line, delivering a spectral resolution $R =$ 40 km s^{-1} (0.65 Å pixel^{-1}). On other occasions, spectra of this line were taken at $R = 15$ km s^{-1} with a thinned CCD. After correcting for fringes and degrading the spectral resolution, these spectra were almost identical to those collected with the infrared array at the same date. Observations in 1992 and 1997–98 were done with a thick CCD that was almost free of fringes, but had a low sensitivity in the blue, which explains the poor coverage of important lines in that spectral range. For wavelengths longer than 6500 Å, telluric absorptions and fringes (in thinned CCDs) were removed by using templates constructed from spectra of bright early-type stars (θ Carinae, ζ Ophiuci or ζ Puppis) observed immediately after or before η Carinae.

For the 2003 event, we also used spectra taken with the spectrographs REOSC ($R = 25$ km s^{-1}) and EBASIM ($R = 7$ km s^{-1}) attached to the 2.15-m CASLEO telescope (Argentina), and spectra taken at CTIO with the 4.0-m Echelle Spetrograph ($R = 8$ km s^{-1}) and at Magellan with the MIKE Spectrograph ($R = 12$ km s^{-1}). For the 1997–98 event, we used spectra collected at La Silla/ESO with CAT-CES ($R = 12$ km s^{-1}). For the 1992 event, we also used spectra collected with the FLASH/HEROS spectrograph attached to the 50-cm telescope (ESO/Chile) with a fibre diameter ∼5 arcsec and spectral resolution $R = 12$ km s^{-1}. On several occasions, we used the FEROS spectrograph attached to the 1.52-m telescope at La Silla to cover the entire optical window at resolution $R =$ 12 km s^{-1}.

Before measuring the spectral features, we degraded the spectra to a dispersion of 0.39 Å pixel^{-1}. This step was not really necessary but it helped facilitate the adoption of the same limits between the narrow and broad components, and positioning of the stellar continuum, when measuring the spectra. Since we adopted the observations collected at the LNA Observatory as a reference, we added data from other sources only in the case where they merged smoothly to the line intensity curve. This criterion was fulfilled by almost all ground-based observations, confirming our expectation that slit-widths in the range 1–3 arcsec would give the same results independent of the position angle of the slit. This happens because the main emitting region is smaller than 1 arcsec and has a huge contrast to the surrounding Homunculus nebula and also because the seeing full width at half-maximum is larger than 1 arcsec, smearing out the emitting region. In a forthcoming paper (on the long-term behaviour of the spectral lines), we will present the complete list of observations from the entire campaign and a table with individual measurements. Fig. 1(a) displays spectra representative of the high- and low-excitation states, showing the disappearance of the high-excitation lines and enhancement of P Cygni absorption profiles during the minimum. Fig. 1(b) shows spectra in the blue for the high-excitation state of 1995 and for the low-excitation state of 1997 and 1970 (see also Damineli et al. 1998 for the full spectral range 3850–11 000 Å).

Spectra from the Space Telescope Imaging Spectrometer (STIS) onboard the *Hubble Space Telescope* are available for the 2003.49 and 1997.95 events, though for consistency we do not include them here since the slit-width is much narrower than used in the ground-based observations, sampling only a part of the inner circumstellar nebulosity. These data are of course important for disentangling stellar from circumstellar variations, and have been more fully described in Nielsen et al. (2007a), Nielsen, Ivarsson & Gull (2007b), Gull, Kober & Nielsen (2006) and Davidson et al. (2005). Since the wind of the primary star is resolved by the STIS slit and the slit's position angle varied in different visits, care must be taken when comparing line profiles from different epochs. This applies to the lower excitation transitions, formed far from the central source(s) that may be subject to spatial asymmetries.

All the data processing and measurements were done in the standard way using IRAF packages. Narrow lines were modelled by Gaussian fitting and deblended from the broad components. Since they are seated on top of broad line profiles, which are themselves variable, we referred their EWs to the local stellar continuum, in order that these measurements correspond to line flux normalized to the local stellar continuum, instead of classical EW. As in the case of EW, this kind of measurement is translated into line flux when multiplied by the stellar continuum flux. Because of this, we use the simple designation of EW in place of normalized line flux. Broad line emission profiles were separated from the narrow components, when they existed, and their EWs and baricentres (for radial velocities) were measured by direct integration along the line profile. Radial velocities are in the heliocentric reference system.

It is difficult to attribute errors to single measurements, as the main source is systematic, not statistical. The spectra were well exposed, in order that photon noise is very low, except in the violet region. The major source of error is linked to the stellar continuum, because of line blendings and changes in relative intensity of line/continuum, as the seeing changes and smears out the central source of emission lines. The random errors can be judged by the smoothness of the curves in line intensity and the plots show that they are small, in general comparable to the size of the symbols in the figures. We minimized the errors by overplotting the spectra and pointing the cursor always in the same position. We must warn, however, that this procedure does not eliminate the systematic errors.

3 DEFINING PHASE 0 FOR THE SPECTROSCOPIC EVENT

A simple method to measure the periodicity of the events is through the disappearance of spectroscopic features like the high-ionization lines or the narrow components of He I (Fig. 2a). In practice, this is difficult because of the following: (i) the time-sampling has been too coarse to pick up the exact time when the feature disappears; (ii) spectroscopic features reach minimum at different times; (iii) minima are usually reached asymptotically for many important spectral features, often taking up to a week to disappear completely; and (iv) when the line EWs are less than ∼100 mÅ, they are difficult to measure, unless the spectra have very high S/N. In addition to producing a large uncertainty in the epoch of the minimum, faint features may not be directly connected to the emitting region, but can be light echoes that fall inside the slit aperture. Moreover, in some cases a very faint blended line remains in emission through the minimum, as in the case of [Ar III] λ7135.

In order to minimize these problems, we restricted our analysis to the phase of steep decline, which lasts for ∼2 weeks, starting ∼3 weeks before complete disappearance. We performed a linear fit, and extrapolated it to zero intensity to determine the time of minimum (Fig. 2b). This procedure is much more robust than other techniques, since it does not require a dense time-sampling along the minimum.

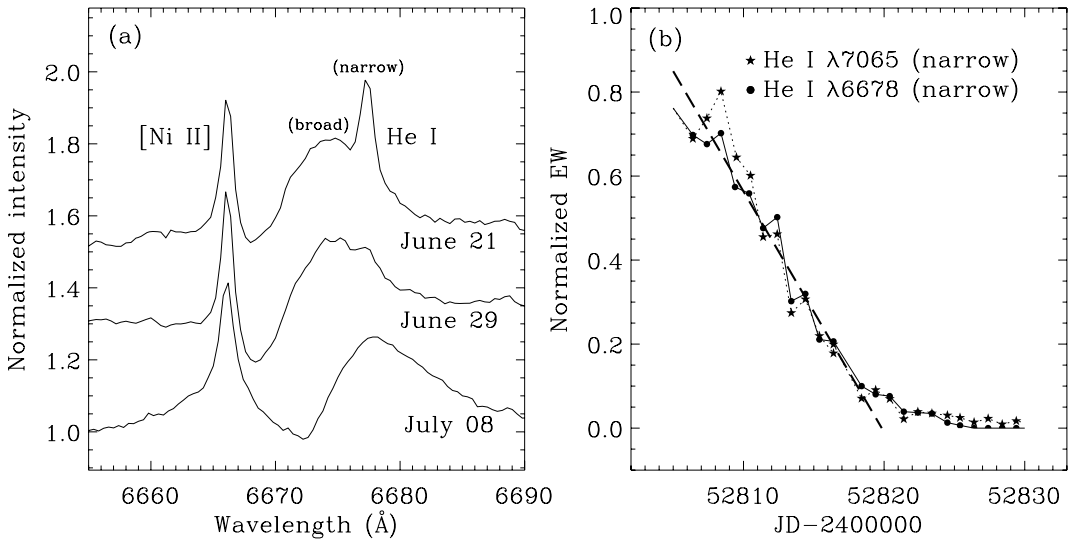

Figure 2. Definition of phase 0 – (a) He I λ6678 line profiles observed along 17 d in 2003, showing the disappearance of the narrow component. (b) The fading phase, showing our method to derive phase 0 (JD 245 2819.8) of He I λ6678 and λ7065 narrow-line components.

It is relatively insensitive to the S/N of the spectrum, and is easily reproducible by other observers. The epoch of minimum, that is, phase 0 (the starting point of the deepest part of the minimum) for the He I λ6678 narrow-line component derived by this method is $T_0 = \text{JD } 245\,2819.8$ (2003 June 29 or 2003.491). Since He I λ6678 is strategic for the spectroscopic event (it has a long observational history, shows clear, easily measured variability and lies in a spectral range with good CCD efficiency), we chose it for our definition of phase 0.

There are two situations for which it is useful to find signatures that indicate the time of phase 0: when examining non-calibrated historical spectra or when trying to track the evolution of an event during a monitoring campaign. As the high-excitation lines are much more variable than the lower excitation lines, and because the spectrum has plenty of lines, it is relatively easy to find line pairs that interchange peak intensity ratio with time. A high-excitation line, as the minimum approaches, decreases until its peak is equal in strength to that of some nearby low-excitation line (in general Fe II or [Fe II]), and we record the date when this occurs. The faster the high-excitation line varies, the more accurate is the determination of the time of change in the line ratio. This happens for dates close to phase 0, when the variability is high, but we were able to find good line pairs up to three months before phase 0 and almost 2 yr after.

We display in Table 1 the time in days for the inversion in peak intensity ratios, relative to phase 0. Negative values represent dates before phase 0 and positive values dates later than phase 0. Entries in column 2 are for the fading phase and in column 3 for the recovering phase, except for He I λ10830, which displays the two ratio inversions in the fading phase. Times are shorter in column 2 than in column 3 due to the fact that the fading phase is fast and the recovering phase is slow. From an examination of data for the last three cycles, we found that times in column 2 are accurate to ∼15 per cent and in column 3 to ∼25 per cent.

In Table 1, we have also listed the line He I λ10830. It has a double peak, like in classical Be stars. The V ('violet') and R ('red') peaks are variable, both in intensity and in their relative strength. For almost the entire 5.5-yr cycle, $R > V$. As the minimum approaches, the R peak starts decreasing faster than the other, in such a manner that 105 d before phase 0 they reach $V = R$, changing to $R < V$ subsequently. The $R < V$ state lasts for almost three months when the rate of fading of the R peak slows down and the V peak starts falling fast. Just 4 d before phase 0, the peaks again reach $V = R$ and return to $R > V$.

Table 1. Time-delays in days, relative to phase 0, when the intensity of line-peaks changes ratio.

Line ratio	Change to <1	Change to > 1
He I 10830 R/V^a peaks	−105	−4
He I 4471/[Fe II] 4475	−46	+550
[S III] 6312/Fe II 6317	−15	+442
[Fe III] 4658/[Fe II] 4640	−17	+358
He I 7065/[Fe II] 7171	−9	+148
He I 6678/[Ni II] 6666	−9	+145
[Fe III] 4658/[Fe II] 4475	−8	+250
[Fe III] 4658/[Fe II] 4665	−5	+168
He I 5876/Na I 5890	0	+18
[N II] 5754/[Fe II] 5746	+1	+79
Fe II 8490/Fe II 8499	+7	+40

[a] 'Red' (R) and 'violet' (V) peak intensity ratio.

4 THE PERIOD LENGTH

There are a number of ways to measure the period length; the best one for spectroscopic data is based on the He I narrow-line components. The EW of this feature remained relatively constant at ∼1500 mÅ for most of cycle #10. About three weeks before phase 0, it began to change fast, declining by ∼25 mÅ d^{-1}. We used this segment of the line-intensity curve to measure the period, applying a scheme of epoch folding and minimization of differences similar to that used by Corcoran (2005). Since we sampled better the fading phase to the minimum, it was sufficient to shift this piece of the line-intensity curve from event #10 until it matched that of event #11 (Fig. 3a) to derive the period. We repeated the same procedure with event #9, getting the best fit for $P = 2026$ d with an uncertainty of 2 d. A careful examination of Fig. 3a, however, indicates that

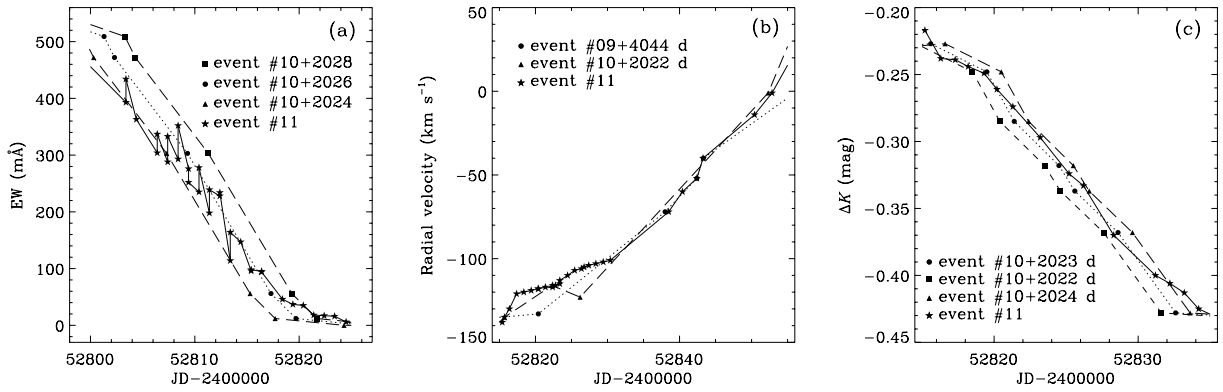

Figure 3. Period length: (a) from the EW He I λ6678 narrow-line component along the latest two events; (b) from radial velocity of the He I λ6678 broad component in the last three events; and (c) from the *K* band by using the method of folding the two latest events and minimizing the residuals.

the slope of the fading phase was steeper during event #10 than in event #11. This is due to secular changing in the line intensity and this is the main source of errors in the period determination by this method.

The broad component of He I λ6678 also changes quickly before the minimum. Its radial velocity decreases slowly in between the events, but three weeks before phase 0 it reverses the trend, and starts to increase. About 4 weeks after phase 0, the radial velocity increases at a rate of $\sim$5 km s^{-1} per day. The steep rise in the radial velocity curve is useful to determine the period length, in the same way as we have done for intensity of the narrow component. This procedure might be more robust than using EWs, since radial velocities are much less affected by the secular variations in intensity. By combining radial velocities from the last three events (events #9, #10 and #11), we derive $P = 2022 \pm 1$ d (Fig. 3b).

Other spectral features were observed, whenever possible, and some of them also were useful for measuring the period length. The total EW of the He I λ10830 line recorded in the last three events gives $P = 2022 \pm 1$ d. The EW of the P Cygni absorption component of the Fe II λ 6455 Å line (also using the last three events) gives $P = 2021 \pm 2$ d and the radial velocity curve of the same line (events #9 and #11) results in $P = 2022 \pm 2$ d. The EW of Si II λ 6347 Å P Cygni component (events #9 and #11) results in $P = 2022 \pm 1$ d.

These periods are in good agreement with $P = 2024 \pm 2$ d derived from X-rays (Corcoran 2005), with $P = 2023 \pm 3$ d from the *K*-band light curve (Whitelock et al. 2004), and with $P = 2021.5 \pm 0.5$ d from the *V* band (van Genderen et al. 2006). We re-derived the periods obtained by those authors, using their published data and applying the technique of folding the pre-minimum branch of two events, events #10 and #11 in the case of Whitelock et al. (2004) and events #7 and #11 in the case of van Genderen et al. (2006). In the case of *V*-band photometry, we combined the light curve of van Genderen et al. (2006) with that of Lajús et al. (2003) in order to get a better definition of the descending branch of the 2003.5 minimum. The derived period was the same as published by van Genderen et al. (2006), but with an uncertainty of 2 d instead of 0.5 d. In the case of near-infrared, Whitelock et al. (2004) used the lower point in the *K*-band minimum. Our procedure of minimization of residuals applied to the *JHKL*-band photometry (Fig. 3c) gave the same period, but with a tighter constraint. It is encouraging to see that the period is robustly defined, independent of the particular choices made by different authors during the measurements (Table 2).

Since there is no reason to suppose that the period length would depend on the particular technique used, we combined all these individual periods to get a mean value to the period. We call it the present-day period ($P_{\rm pres}$) to differentiate from that determined from historical observations. Since the systematic errors may be more important than statistical errors, we report the uncertainty in the period as a simple standard deviation.

Table 2. Period length in days from different spectral regions.

Period ± error	Spectral feature or pass-band
2026 ± 2	He I 6678 narrow component EW
2024 ± 2	X-rays
2023 ± 1	*J* band
2023 ± 1	*H* band
2023 ± 1	*K* band
2023 ± 2	*L* band
2022 ± 2	Fe II 6455 P Cygni absolute radial velocity
2022 ± 1	Si II 6347 EW
2022 ± 1	He I 6678 broad radial velocity
2022 ± 1	He I 10830 EW
2021.5 ± 2	*V* band
2021 ± 2	Fe II 6455 P Cygni absolute EW
2022.7 ± 1.3	Average ± standard deviation

$$P_{\rm pres} = 2022.7 \pm 1.3 \text{ d} \quad \text{or} \quad P_{\rm pres} = 5.538 \pm 0.004 \text{ yr}.$$

Regarding the times of phase 0, there is no reason to expect that different features give the same epoch, since they are produced in a variety of regions – in the stellar winds, in the WWC and in the circumstellar material. Since we are dealing mostly with spectroscopic lines, we define, for reasons discussed earlier, phase 0 of the spectroscopic events from the disappearance of the He I narrow-line intensity. This yields the following ephemeris:

$$\text{JD(phase 0)} = 245\,2819.8 \pm 0.5 + (2022.7 \pm 1.3\,\text{d})E.$$

The uncertainty is only 0.07 per cent of the period length, which enables us to accurately predict the time of phase 0 of the next spectroscopic event: JD 245 4842.5 ± 2 (2009 January 9–13).

5 STABILITY OF THE PERIOD

An important question is the long-term stability of the period, since the companion stars are losing mass at high rates and tidally interact during the periastron passages. In addition, the primary star could be a fast rotator – as indicated by its dense polar wind (Smith et al. 2003; van Boeckel et al. 2005; Weigelt et al. 2007) – and the specific

Table 3. Period derived from epochs of predicted and observed minima.

Cycle	Pred. JD (^{b})	Predicted (Date)	Observed (Date)	P (d)
#1	325 92.8	1948 February 11	1948 April 19	>2015.9
#2	346 15.5	1953 October 26	1953 June 28^a	<2029.3
#2	”	”	1953 December 30	>2009
#3	366 38.2	1959 March 11	1959 May 14	>2014.4
#4	386 60.9	1964 September 23	1965 February 15	>2001.9
#5	406 83.6	1970 April 07	1970 May 17	>2016.0
#7	447 29.0	1981 May 04	1981 May 21	>2018.6
#8	467 51.7	1986 November 17	1987 January 15	>2003.1
#9	487 74.40	1992 June 01	1992 May 31	–
#10	507 97.10	1997 December 15	1997 December 12	–

^{a}Intermediate excitation. ^{b}JD +240 0000.

angular momentum may be changing continuously. The coupling of rotational and orbital angular momentum may lead to an increase in the orbital period. A period derived from data encompassing many cycles may be hiding such variations. The only way to tackle this question is by comparing the present-day period (measured from the last few events) with the average period ($P_{\rm avg}$), derived from the events recorded in the past 60 yr.

We looked at the events reported by Feast et al. (2001). In case the spectrum was in low-excitation state, we assumed that it had just reached the minimum and so was at phase 0. As a matter of fact, phase 0 must have occurred already at some time before the observation, in order that a period based on that record would underestimate the period. The average period, or more precisely a lower limit to it, is obtained from the time-interval between that date and the last recorded minimum (2003.49) divided by the number of cycles. The derived average periods are presented in column 5 of Table 3. We excluded the last three events, since they were used to derive the present-day period. The dates of observed minima in Table 3 (column 4) were taken from Feast et al. (2001), except for the observation on 1970 May 17. This spectrum (taken at CTIO) was recorded by Virpi Niemela and indicates that phase 0 occurred at least 8 d before Thackeray's observation reported by Feast et al. (2001). The CTIO logbook reports that spectra were taken by Barry Lasker a day before phase 0 of the 1970 event (April 6), which could lead to a very tight constraint on the period, but unfortunately we were not able to locate that spectral plate.

The observation made on 1948 April 19 gives $P_{\rm avg} > 2015.9$ d and that of 1981 May 21 gives $P_{\rm avg} > 2018.6$ d. We can constrain the period length also from the other side. A maximum period may be derived when a particular observation was made before phase 0. This is the case for the observation made on 1953 June 28, when the star was approaching the minimum, but was still in an intermediate phase, which gives $P_{\rm avg} < 2029.3$ d. The average period is thus constrained to

$$2029.3 > P_{\rm avg} > 2018.6 \text{ d}.$$

The stability of the period can be obtained from the difference between the present-day period and the average period, taking into account that $P_{\rm avg}$ refers to half of the cycles involved. The spectrum taken on 1953 June 28 indicates that the period cannot have decreased by more than 1.4 d cycle^{-1} and that of 1948 April 19 implies that it cannot have increased by more than 1.4 d cycle^{-1}.

We have another way to constrain the average period using quantitative information of the first event in 1948. Gaviola (1953) reported that [N II] λ5754 was fainter than [Fe II] λ5746, which places the date of the observation in a particular range inside the low-excitation event. An examination of recent events indicates that before phase 0, [N II] is much stronger than the neighbouring [Fe II] line. The [N II] line decreases quickly, in contrast to [Fe II] which undergoes small and slow changes. Both features reach equal intensity 0.7 d after phase 0, as can be seen in Fig, 4(a), where variations during event #11 are displayed. The [N II] line remains fainter than [Fe II] for a subsequent 78 d. This can be seen in Fig. 4(b), which combines measurements made in the last three events. The ratio of these two lines is not sensitive to the slit-width or to the spectral resolution, as long as they are kept <4 arcsec or $R > 2000$, respectively. The fact that the 1948 observation was done <78 d later than phase 0, combined with the epoch of the 2003.49 minimum results in

$$P_{\rm avg} = 2020 \pm 4 \text{ d}.$$

This period is compatible with that derived in the present-day data. Taking into account that the average was taken between

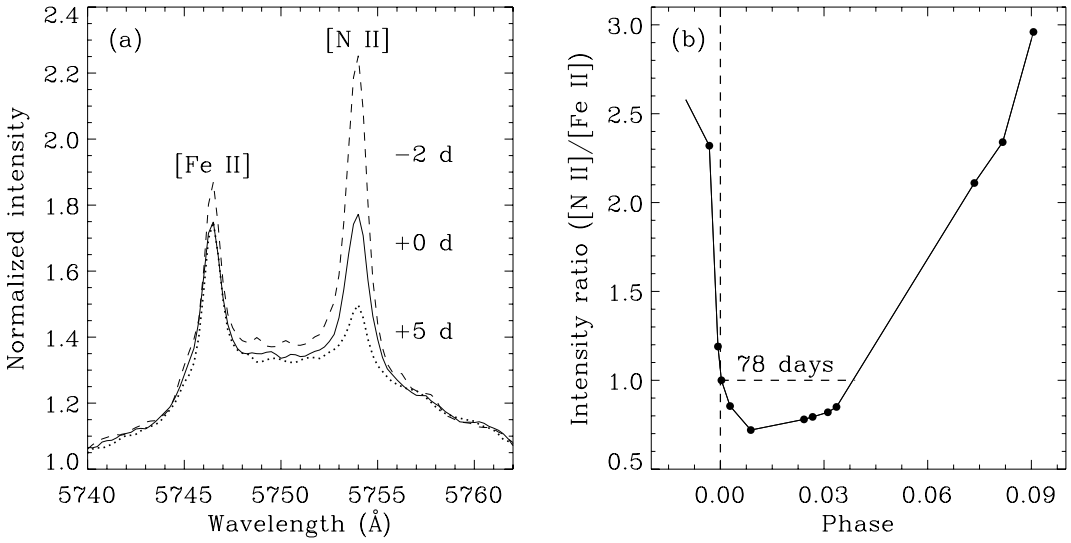

Figure 4. Relative intensities of [N II] λ5754 and [Fe II] λ5746 – (a) line profile variations. The labels on the right-hand side of the [N II] peak indicate days from phase 0 of the 2003.49 event. (b) Ratio between line peaks, indicating that [N II]/[Fe II] < 1.0 starts at phase 0 and lasts for 78 d during the minimum.

10 cycles, it could not have changed by more than 1.5 d cycle^{-1}, in close agreement with 1.4 d cycle^{-1} derived before. The constraint to the period change is

$$-0.0007 < \frac{\Delta P}{P} < +0.0007.$$

This confirms previous claims of strict periodicity by Damineli (1996), Damineli et al. (2000) and Feast et al. (2001) implying that the low-excitation events are only understandable in the binary scenario. It is also consistent with the period change expected because of mass loss from the primary star. Simple considerations show that $\dot{P}/P = \alpha \dot{M}/M$, where α is a constant of the order of unity (Khaliullin 1974). Ignoring changes in eccentricity, we find

$$\dot{P} = 0.11\alpha \left(\frac{\dot{M}}{10^{-3}\,\mathrm{M_\odot\,yr^{-1}}}\right)\left(\frac{100\,\mathrm{M_\odot}}{M}\right)\ \mathrm{d\,cycle^{-1}}.$$

This is fully consistent with the observed upper limit.

6 WERE THE PEAKS IN THE GIANT ERUPTION PRODUCED BY PERIASTRON PASSAGES?

Damineli (1996) pointed out that the three most-pronounced peaks observed in 1827–43 were in close coincidence with the predicted times of phase 0, when using the period $P = 2014$ d. Frew (2004) also noted that the 'Lesser Eruption' which began on 1887.5 was within a few months of phase 0. When using the new period, derived in this work ($P = 2022.7$ d), the 1827.087 peak is now at phase 0.15, that of 1837.967 is at phase 0.13, and that of 1843.3 at phase 0.05 (Frew 2004), while the 1887.5 event corresponds to a phase of 0.96. The correlation between peaks and the start of the spectroscopic events worsens with the new ephemeris. However, an exact correlation between the times of the peaks and phase 0 is not really relevant, since the time-sampling of the visual light curve was not very dense and the real maxima could have been missed by the observers. Moreover, if the mechanism that produced those peaks is the same as the one that produces the broad maxima observed presently in the near-infrared light curve, the lack of coincidence with phase 0 would not be a surprise. As reported by Whitelock et al. (2004), the *JHK* light curves present maxima around phase 0, but not in exact coincidence. These near-infrared peaks are quasi-periodic and may remain in high state for up to 3 yr, depending on the wavelength. Although the near-infrared light curve is anti-correlated with the radio flux, it still can be explained as free–free emission if optical depth effects are taken into account (Whitelock et al. 2004).

In the *V* band, the maxima associated with the periastron are inconspicuous, as compared to those in the near-infrared. Could they have been more pronounced during the giant eruptions of the 19th century? There is no reason to believe so, as η Carinae was much brighter in the optical than it is now, diminishing the contrast between the quasi-periodic maxima and the underlying stellar light. However, this is an unsafe terrain, as we do not know what mechanism produced the pronounced peaks during the giant eruption.

Recent estimates of the Homunculus mass suggest that more than 10 $\mathrm{M_\odot}$ of material was ejected during the great eruption (Smith et al. 2003). Given the larger mass loss that occurred in the giant eruption, it is likely that the orbital parameters changed substantially during the great eruption, and thus it is not surprising that there is not a one-to-one correspondence between orbital phase and the pronounced peaks observed in 1827–43, even if they were a result of a binary interaction near periastron.

7 DISCUSSION AND CONCLUSIONS

We presented a homogeneous set of spectra covering events #9 (1992.42), #10 (1997.95) and #11 (2003.49). We derived the period by measuring intensities of narrow lines (Weigelt blobs) and broad emission lines (stellar wind) and radial velocity variations from broad line components. These data, and others collected from the literature, enable an accurate determination of the period $P_{\rm pres} = 2022.7 \pm 1.3$ d. An average period encompassing the past 11 cycles was found to be $P_{\rm avg} = 2020 \pm 4$ d, compatible with the present-day period. The period change is smaller than 1.5 d cycle^{-1} along the last half century.

It is difficult to imagine any mechanism other than orbital motion which could maintain such a high stability, while allowing individual features to show the distinct light curves that are observed. No luminous unstable star is expected to follow such a precise clock. Even if it is conceivable that a shell ejection could be involved in the periodic events, it should be triggered by the periastron passage, when the secondary star approaches the primary to a few stellar radii. However, in a forthcoming paper, we show that the event starts when the secondary star is still near apastron.

We must expect that the period is drifting, since the stars are losing mass, they interact strongly as they get very close at periastron and the primary star appears to be a fast rotator. The period changes have been $\Delta P/P < 1/1000$ along the last 60 yr, which is consistent with the observed mass-loss rate.

The situation is different for the eruptions of 1843 and 1890, when a considerable amount of matter was removed from the primary star in brief episodes. However, the relation between the pronounced peaks observed during the great eruption and periastron passages continues to be unknown. This is because the coincidence is not perfect, and because the peaks might not be strictly periodic but could still be associated with periastron passages, as seen presently in the near-infrared light curves.

From the disappearance of the He I λ6678 narrow component, we determined the epoch of the start of the minimum to be $T_0 =$ JD 245 2819.8. The procedure to define the minimum requires fitting and extrapolating the line-intensity variation along the descending part of the line-intensity curve, in the two weeks preceding the minimum intensity. Because of this definition, and since the starting time of the minimum is different from line to line, this definition is arbitrary and has no physical meaning. However, it is robust and demands only a few observations along ∼3 weeks before the complete disappearance of the feature. Importantly, the time-delay for all other features to reach the minimum is well known.

The next minimum is predicted to start on 2009 January 11 (±2 d). This will be the best event since 1948 for ground-based observations, since its central core fits entirely in the good observing season. The next favourable event will not occur before 2020. In order to improve the results presented in this work, daily observations should be made along a month starting on 2008 December 20.

ACKNOWLEDGMENTS

We thank J. E. Steiner and T. Gull for their comments on this draft. AD, JHG and MT thank FAPESP and CNPq for continuing support. Financial support from PIP-CONICET No. 5697 is acknowledged by JA. DJH acknowledges partial support from HST AR-10957.

REFERENCES

Abraham Z., Falçeta-Gonçalves D., Dominici T. P., Nyman L.-Å D. P., McAulaife F., Caproni A., Jatenco-Pereira V., 2005, A&A, 437, 977

Corcoran M. F., 2005, AJ, 129, 2018

Damineli A., 1996, ApJ, 460, L49

Damineli A., Conti P. S., Lopes D. F., 1997, New Astron., 2, 107

Damineli A., Stahl O., Kaufer A., Wolf B., Quast G., Lopes D. F., 1998, A&AS, 133, 299

Damineli A., Kaufer A., Wolf B., Stahl O., Lopes D. F., de Araújo F. X., 2000, ApJ, 528, L101

Davidson K., Ebbets D., Weigelt G., Humphreys R. M., Hajian A. R., Walborn N. R., Rosa M., 1995, ApJ, 109, 1784

Davidson K. et al., 2005, AJ, 129, 900

Duncan R. A., White S. M., 2003, MNRAS, 338, 425

Feast M., Whitelock P., Marang F., 2001, MNRAS, 322, 741

Frew D. J., 2004, JAD, 10, 6

Gaviola E., 1953, ApJ, 118, 234

Groh J. H., Damineli A., 2004, Inf. Bull. Var. Stars 5492

Gull T. R., Kober G. V., Nielsen K. E., 2006, ApJS, 163, 173

Hamaguchi K. et al., 2007, ApJ, 663, 522

Hillier D. J., Allen D. A., 1992, A&A, 262, 153

Khaliullin Kh. F., 1974, Astron. Zh., 51, 395 (1974, Sov. Astron., 18, 229)

Lajús E. F., Gamen R., Schwartz M., S alerno N., Llinares C., Fariña C., Amorín R., Niemela V., 2003, IBVS 5477

Martin J. C., Davidson K., Humphreys R. M., Hillier D. J., Ishibashi K., 2006, ApJ, 640, 474

Nielsen K. E., Corcoran M. F., Gull T. R., Hillier D. J., Hamaguchi K., Ivarsson S., Lindler D. J., 2007a, ApJ, 660, 669

Nielsen K. E., Ivarsson S., Gull T. R., 2007b, ApJS, 168, 289

Rodgers A. W., Searle L., 1967, MNRAS, 135, 99

Smith N., Gehrz R. D., Hinz P. M., Hoffmann W. F., Hora J. L., Mamajek E. E., Meyer M. R., 2003, AJ, 125, 1458

Steiner J. E., Damineli A., 2004, ApJ, 612, L133

Thackeray A. D., 1953, MNRAS, 113, 211

Thackeray A. D., 1967, MNRAS, 135, 51

van Boeckel R. et al., 2003, A&A, 410, L37

van Genderen A. M., Sterken C., Allen W. H., Walker W. S. G., 2006, JAD, 12, 3

Weigelt G., Ebersberger J., 1986, A&A, 163, L5

Weigelt G. et al., 2007, A&A, 464, 87

Whitelock P., Feast M. W., Koen C., Roberts G., Carter B. S., 1994, MNRAS, 270, 364

Whitelock P. A., Feast M. W., Marang F., Breedt E., 2004, MNRAS, 352, 447

Zanella R., Wolf B., Stahl O., 1984, A&A, 137, 79

This paper has been typeset from a TEX/LATEX file prepared by the author.